Synthesis of cyclic peptides as bioconjugation platforms

Peterse, E.

6

Summary and future prospects

Cyclic peptides encompass a major class of macrocylic compounds, varying widely in structure, ring size, functional group patterns and biological activities. The defining characteristic of macrocycles are their cyclic structure consisting of twelve or more atoms. During the early days of antibiotic research extensive investigations were conducted on cyclic peptides leading to a vast resource of antimicrobial compounds. In recent years, interest in peptidic macrocycles as therapeutics has been renewed as these compounds occupy a middle space between small-molecule drugs and large pharmaceutical agents (biologicals) such as proteins

and antibody-drug conjugates. Cyclic peptides have also seen widespread usage as a multifunctional platform by utilizing a peptide template that serves as a structural motif onto which several molecular entities can be attached.

Macrocyclization is the key step in the synthesis of cyclic peptides and **Chapter 1** provides an overview of the main strategies employed. To exemplify, syntheses of several bioactive peptides are described utilizing these strategies. The applications of cyclic peptides as multifunctional platforms are discussed as well and representative examples are given.

The attachment of lysine ε-amines or ornithine δ-amines to resins most commonly involve the usage or synthesis of an activated electrophilic resin. **Chapter 2** describes the establishment of a method to anchor the lysine and ornithine side-chains using the nucleophilic para-hydroxymethylphenyloxy (Wang) linker on a TentaGel resin through a carbamate linkage. When compared to the linkage of the respective C-terminus, the properties of the linker remain unaffected as exposure to trifluoroacetic acid liberates the amine accompanied by the formation of carbon dioxide. The method involves the formation of an isocyanate which was achieved through treatment of the *N*-Boc carbamate with the oxaphilic Hendrickson's reagent. The coupling of the isocyanate to Wang-type resins was found to be efficiently catalyzed by dibutyltin dilaurate and zirconium(IV) acetylacetonate. With these methods, four head-to-tail cyclic peptides were synthesized in yields and purities comparable to those reported in literature.

It would be of interest to widen the scope of this method to paint a more complete picture. Since the equivalents of the catalysts has not yet been varied, it would be interesting to find out the minimum amounts of catalysts that could still efficiently catalyze the reaction. As the choice of base was also found to be influential, investigating different bases would be a logical next step as well. The two tested bases, *N*-methylmorpholine and 1-methylimidazole, were reported to be catalysts itself for the transformation and attempting the coupling with a non-catalytic base might achieve better synergy. Possible bases are limited to ensure Fmoc compatibility, but the sterically hindered 2,6-lutidine would be an interesting candidate. Additionally, the number of different resins can be increased. The method has been only tested on TentaGel resins, which is a graft copolymer of weakly cross-linked polystyrene and linear polyethylene glycol.[1] Polystyrene-based resins as well as resins comprised of only polyethylene glycol, such as the PEGA and

ChemMatrix resins, would be valuable additions.[2–4] The inclusion of additional amines, such as 2,4-diaminobutyric acid, would open up the possibility of synthesizing a wider variety of cyclic peptides. Interesting peptides include the head-to-side-chain cyclic peptide polymyxin B2 **1** and the cyclic tetradecapeptide murepavadin **2** (*Figure 1*).

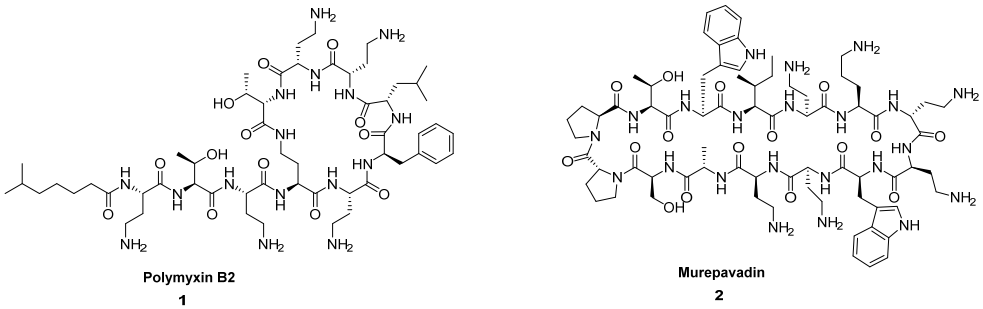

Figure 1. A wider variety of cyclic peptides that could be synthesized include polymyxin B2 **1** and murepavadin **2**.

There have been recent reports investigating the synergystic effects of various (conjugated) Toll-like receptor (TLR) ligands. **Chapter 3** describes the synthesis of a platform to probe the influence of the spatial positioning of a pair of TLR agonists on their immunogenicity. Advantage was taken of the cyclodecapeptide gramicidin S which presents amino acid side-chains into opposite planes owing to its secondary structure. Three gramicidin S scaffolds were synthesized that orient the amine functionalities into different directions. To facilitate swift and clean attachment of the TLR ligands, the amines were equipped with a maleimide group and a BCN moiety. TLR2, 7 and 9 ligands were synthesized with a complementary reactive group (thiol or azide) creating nine possible combinations of ligands and orientation. To accommodate on-resin installation of the BCN moiety, the method developed in Chapter 2 was expanded to the TentaGel S AC resin and the peptide cleavage and purification method were optimized. In the future, RP-HPLC purification of the cyclopeptides carrying the BCN group should be carried out with ammonium acetate instead of TFA to avoid alkyne hydration.

Chapter 4 describes the expansion of the platform in Chapter 3 to allow presentation of three different TLR ligands. Adjustments were made to install the third ligand *via* tetrazine/norbornene ligation by substituting the BCN group with the bulky DBCO moiety preventing cross-reaction of the tetrazine. Two gramicidin S-based scaffolds were synthesized carrying three amino functionalities in different orientations. The

norbornene and DBCO groups were installed on-resin which required an additional protected amine during synthesis of the peptide. The Tfa group proved effective and could be removed by treatment with ammonia in methanol under microwave irradiation at elevated temperatures. To accompany the new ligation, a TLR7 ligand carrying a tetrazine was synthesized as well as an adapter molecule for the TLR9 agonist. With these molecules in hand, three combinations of ligands and orientations are possible.

The main priority moving forward is conjugation of the TLR agonists to the scaffolds. As there have been several reports of cross-reactivity between the thiol and alkyne functionalities, the best option would be sequential conjugation.[5,6] Counterintuitively, the group of Plückthun achieved higher yields of protein-protein ligation when performing the thiol-maleimide ligation first which they attribute to the longer reaction times required for the azide-alkyne cycloaddition leading to maleimide hydrolysis and other side-reactions.[7] Since these molecules are several magnitudes smaller, both sequences should be attempted. Following literature precedent, the alkyne-azide cycloaddition and tetrazine/norbornene ligation could be performed simultaneously as they are mutually orthogonal.[8–10] As for the biological evaluation of the linked TLR agonists, it would be of interest to follow the example set by the group of Esser-Kahn to allow for comparison.[11] In their evaluation of linked triagonists, they examined activation of the transcription factor NF-κB, which leads to cytokine production, as a measure of synergistic activity as well as activation of interferon stimulatory genes. They also build a cytokine profile by analyzing cytokine concentrations, in particular IL-12p70, TNF-α, IFN-γ, IL-6, IL-10 and CCL2.

To create a more diverse library, it would be of interest to increase the number of TLR ligands. The most sensible additions would be the pyrimido[5,4-*b*]indole **3**, a TLR4 ligand, and the diacylated Pam_2Cys **4** that is an agonist for TLR2/6 (*Figure* 2).[12,13] It would also be interesting to widen the scope to more ligands of pattern recognition receptors. The NOD2 agonist muramyl dipeptide **5** would be a valuable addition as there have been promising results with TLR2/NOD2 dual ligands.[14,15] Benzothiazole compound **6** was found by Gale and co-workers to activate the transcription factor interferon regulatory factor 3 (IRF3) in the RIG-I-like receptor (RLR) signaling pathway and would be an interesting addition in the future.[16] Lastly, diamidobenzimidazole **7** has been recently identified as an agonist for stimulator of

interferon genes (STING) eliciting a type-I interferon response and would make an interesting inclusion in the library.[17]

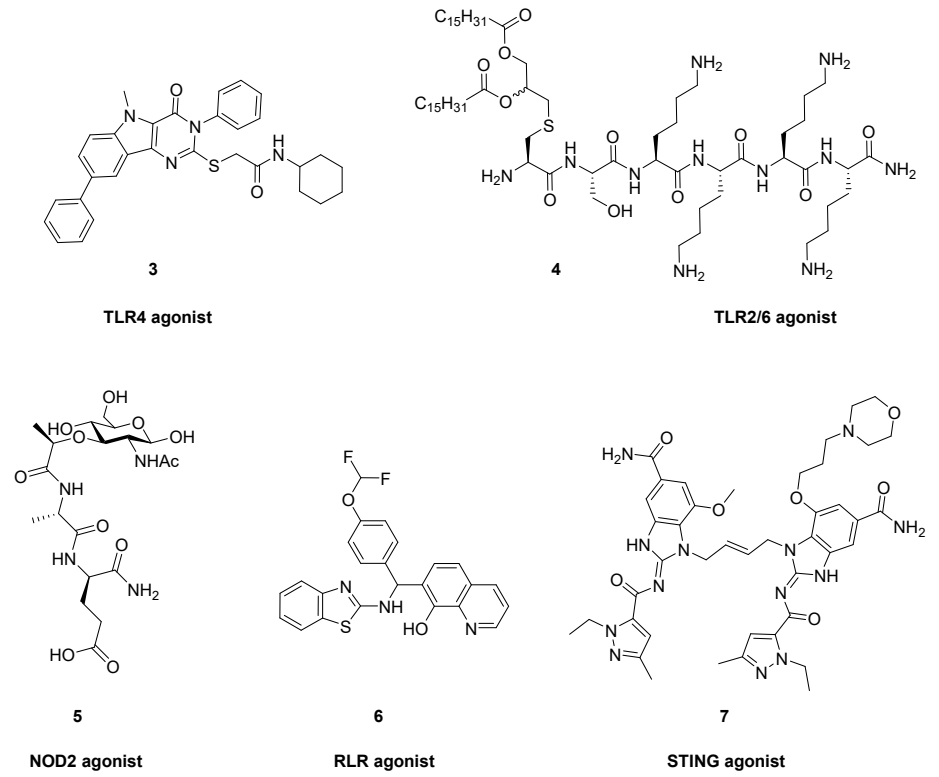

Figure 2. Possible agonists of pattern recognition receptors to expand the library created in Chapters 3 and 4.

Chapter 5 describes the synthesis of a fusion protein utilizing a chemical conjugation strategy. A linker system was designed that placed the emphasis on late-stage derivatization of the individual proteins. Anti-PD1 and anti-CD4 VHH antibodies were genetically engineered with a C-terminal cysteine for conjugation purposes and were obtained in good purities. A two-component linker system was synthesized to facilitate late-stage fusion. One linker consisted of an iodoacetamide group as a complement to the thiol group and an azide moiety for a SPAAC ligation. The complementary linker was equipped with a maleimide for thiol conjugation and the strained cycloalkyne BCN as the ligation partner for the azide and were linked together by an ethylene glycol spacer. The linkers were successfully conjugated to anti-PD1 VHH antibodies and a preliminary investigation was conducted on the

SPAAC ligation which saw formation of the fusion protein, but further optimization is needed.

The first step for optimization could be to apply the optimal conditions found by Schiffelers and co-workers for conjugating a 20 kDa poly-ethylene glycol to a VHH antibody *via* a SPAAC ligation, which includes a higher temperature (50 °C) and a 3:1 ratio of alkyne to azide.[18] Another adjustment that could be made is increasing the length of the linkers. The design of the BCN linker allows for facile prolongation by incorporating more ethylene glycol spacers during the solid-phase synthesis. Increasing the length of the azido linker requires more attention, but has been achieved as well (*Figure 3*). After obtaining amine **8**, the compound was reacted with the ethylene glycol spacer utilizing Castro's reagent and DIPEA to afford Fmoc-protected amine **9** in 44% yield. Fmoc deprotection was achieved with 1,8-diazabicyclo[5.4.0]undec-7-ene (DBU) and *n*-octanethiol as the scavenger giving amine **10** in 96% yield. The iodoacetamide was installed in a similar manner as described in Chapter 2 and compound **11** was obtained in 56% yield over two steps.

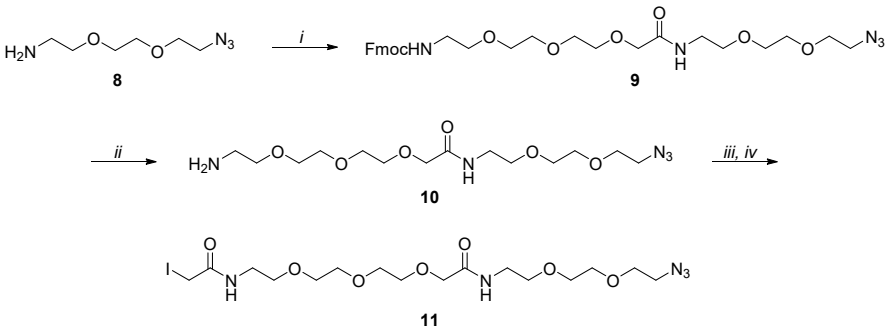

Figure 3. Reagents and conditions: (*i*) Ethylene glycol building block, BOP, DIPEA, DMF, rt, 4 hrs, 44% (*ii*): DBU, *n*-octanethiol, THF, rt, 36 hrs, 96% (*iii*) Chloroacetyl chloride, Et_3N, DMF, 0 °C, 2.5 hrs, 77% (*iv*): NaI, acetone, rt, 48 hrs, 73%.

A limitation of the current approach is the reliance on cysteine for the conjugation of the linkers to the protein. When additional cysteines are present on the protein selectivity cannot be guaranteed. An alternative would be the utilization of ligation enzymes, such as sortase A and butelase.[19,20] However, that would require the engineering of different linkers on each protein hampering the goal of late-stage derivatization. Another option would be the site-specific cysteine conjugation developed by the group of Pentelute (*Figure 4*).[21] A four-amino-acid sequence (Phe-Cys-Pro-Phe) tunes the reactivity of the cysteine thiol enabling site-selective

conjugation with perfluoroaromatic reagents and the addition of ammonium sulfate accelerates the reaction.[22] This motif could be engineered at the C-termini of the antibodies while the perfluoroaromatic group could be installed instead of the maleimide and iodoacetamide functionalities. The use of this conjugation could be the basis of a more general fusion protein approach.

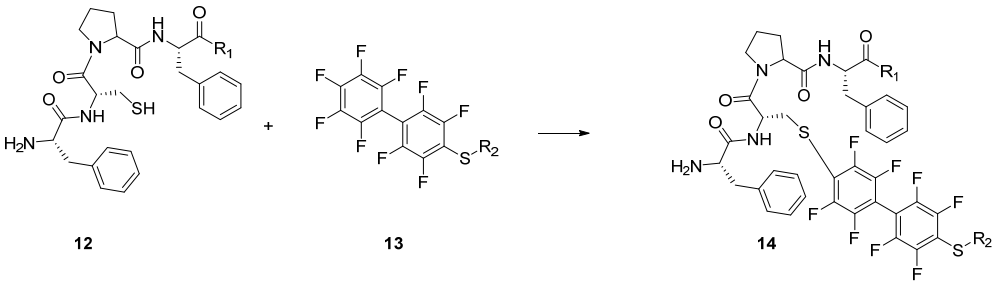

Figure 4. The site-selective cysteine conjugation of a four-amino-acid sequence with perfluoroaromatic reagents developed by the group of Pentelute.

General information

Materials, reactions and purification

Standard Fmoc-amino acids and resins for solid-phase peptide synthesis (SPPS), amino acids for solution-phase synthesis and peptide coupling reagents 2-(6-chloro-1*H*-benzotriazole-1-yl)-1,1,3,3-tetramethyluronium hexafluorophosphate (HCTU), *N*,*N*'-diisopropylcarbodiimide (DIC), 1-ethyl-3-(3-dimethylaminopropyl) carbodiimide hydrochloride (EDC), ethyl cyano(hydroxyimino)acetate (Oxyma Pure) and 1-hydroxybenzotriazole (HOBt) were purchased from Novabiochem or Sigma-Aldrich. The resin TentaGel S RAM (0.25 mmol/g) was bought from Rapp Polymere. All other chemicals were purchased from Acros, Sigma Aldrich, VWR, Fluka, Merck and Fisher Scientific and used as received unless stated otherwise. Tetrahydrofuran (THF), *N*,*N*-dimethylformamide (DMF), dichloromethane (DCM), 1,4-dioxane and toluene were stored over molecular sieves before use. Commercially available ACS grade solvents were used for column chromatography without any further purification, except for toluene and ethyl acetate which were distilled prior to use. All reactions were carried out under a nitrogen atmosphere, unless indicated otherwise. Reaction progress and chromatography fractions were monitored by thin layer chromatography (TLC) on silica-gel-coated aluminium sheets with a F254 fluorescent indicator purchased from Merck (Silica gel 60 F_{254}). Visualization was achieved by UV absorption by fluorescence quenching, permanganate stain (4 g $KMnO_4$ and 2 g K_2CO_3 in 200 mL of H_2O), ninhydrin stain (0.6 g ninhydrin and 10 mL acetic acid in 200 mL ethanol). Silica gel column chromatography was performed using Screening Devices silica gel 60 (particle size of 40 – 63 μm, pore diameter of 60 Å) with the indicated eluent. Analytical reversed-phase high-performance liquid chromatography (RP-HPLC) was performed on a Thermo Finnigan Surveyor HPLC system with a Phenomenex Gemini C_{18} column (4.6 mm x 50 mm, 3 μm particle size) with a flow rate of 1 mL/min and a solvent gradient of 10-90% solvent B over 8 min coupled to a LCQ Advantage Max (Thermo Finnigan) ion-trap spectrometer (ESI^+). Preparative RP-HPLC was performed with a GX-281 Liquid Handler and a 331 and 332-H2 primary and secondary solvent pump respectively with a Phenomenex Gemini C_{18} or C_4 column (250 x 10.0 mm, 3 μm particle size) with a flow rate of 5 mL/min and solvent gradients as described for each compound. HPLC solvent compositions: solvent A is 0.1% (v/v) TFA in H_2O; solvent B is MeCN. Preparative RP-HPLC was also performed on an Agilent 1200 HPLC system coupled to a 6130 Quadrupole Mass Spectrometer using a Nucleodur C_{18} Gravity column (250 x 10.0 mm, 5 μm particle size) with a flow rate of 5 mL/min and a gradient over 12 min. as described for each compound. HPLC solvent composition: solvent A is 0.2% (v/v) TFA in H_2O and solvent B is MeCN. All HPLC solvents were filtered with a Millipore filtration system equipped with a 0.22 μm nylon membrane filter prior to use.

Characterization

Nuclear magnetic resonance (^1H and ^{13}C APT NMR) spectra were recorded on a Brüker DPX-300, Brüker AV-400, Brüker DMX-400, Brüker AV-500 or Brüker DMX-600 in the given solvent. Chemical shifts are reported in parts per million (ppm) with the residual solvent or tetramethylsilane (0 ppm) as reference. High-resolution mass spectrometry (HRMS) analysis was performed with a Thermo Finnigan LTQ Orbitrap mass spectrometer equipped with an electronspray ion source in positive mode (source voltage 3.5 kV, sheath gas flow 10 ml/min, capillary temperature 250 °C) with resolution R = 60000 at m/z 400 (mass range m/z = 150 – 2000) and dioctyl phthalate (m/z = 391.28428) as a "lock mass". The high-resolution mass spectrometer was calibrated prior to measurements with a Thermo Finnigan calibration mixture. Nominal and exact m/z values are reported in daltons.

(9*H*-fluoren-9-yl)methyl (1-azido-10-oxo-3,6,12,15,18-pentaoxa-9-azaicosan-20-yl)carbamate

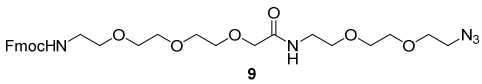

9

An oven-dried 50 mL flask was charged with ethylene glycol spacer bearing the carboxylic acid (1.1 g, 2.5 mmol, 1.0 equiv.). Benzotriazol-1-yloxytris(dimethylamino)phosphonium hexafluorophosphate (BOP) (1.4 g, 3.2 mmol, 1.3 equiv.) was added and the mixture was dissolved in anhydrous DMF (13 mL, 0.20 M). DIPEA (1.3 mL, 7.5 mmol, 3.0 equiv.) and 2-(2-(2-azidoethoxy)ethoxy)ethan-1-amine (0.57 g, 3.3 mmol, 1.3 equiv.) were added and the mixture was stirred for 4 hours. The mixture was concentrated by co-evaporation with *n*-heptane and purified by silica gel column chromatography (7:3, DCM – MeCN) to yield compound **9** (0.64 g, 1.1 mmol, 44%) as a colourless oil.

^{1}H NMR (400 MHz, $CDCl_3$) δ 7.66 (d, *J* = 7.5 Hz, 2H, C*H*-arom), 7.52 (d, *J* = 7.5 Hz, 2H, C*H*-arom), 7.29 (t, *J* = 7.5 Hz, 2H, C*H*-arom), 7.21 (t, *J* = 7.4 Hz, 2H, C*H*-arom), 7.14 (t, *J* = 5.8 Hz, 1H, N*H*), 5.81 (t, J = 5.7 Hz, 1H, N*H*Fmoc), 4.32 (d, *J* = 6.9 Hz, 2H, CH_2-Fmoc), 4.11 (t, *J* = 6.8 Hz, 1H, C*H*-Fmoc), 3.92 (s, 2H, CH_2(C=O)), 3.59 – 3.25 (m, 24H, OCH_2, CH_2N_3, CH_2NH). ^{13}C NMR (101 MHz, $CDCl_3$) δ 169.9 (*C*=O), 156.3 (*C*=O), 143.71 (*Cq*-arom), 141.0 (*Cq*-arom), 127.4 (*C*H-arom), 126.8 (*C*H-arom), 124.8 (*C*H-arom), 119.7 (*C*H-arom), 70.5 (OCH_2), 70.2 (OCH_2), 70.1 (OCH_2), 70.1 (OCH_2), 70.0 (OCH_2), 69.9 (OCH_2), 69.7 (OCH_2), 69.6 (OCH_2), 69.5 (CH_2(C=O)), 66.1 (CH_2-Fmoc), 50.3 (CH_2N_3), 47.0 (CH-Fmoc), 40.6 (CH_2NH), 38.3 (CH_2NH).

***N*-(1-azido-10-oxo-3,6,12,15,18-pentaoxa-9-azaicosan-20-yl)-2-chloroacetamide**

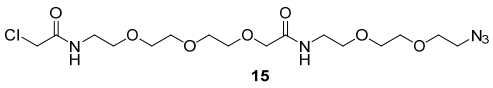

15

Compound **9** (0.52 g, 0.89 mmol, 1.0 equiv.) was dissolved in anhydrous THF (7.7 mL, 0.12 M). *n*-Octanethiol (1.5 mL, 8.8 mmol, 10 equiv.) was added followed by dropwise addition of 1,8-diazabicyclo[5.4.0]undec-7-ene (DBU) in THF (1.0 mL, 88 mM). The mixture was allowed to stir for 36 hours. The mixture was evaporated and the residue was dissolved in toluene (5.0 mL). H_2O (5.0 mL) was added and the aqueous layer was separated. The organic layer was extracted with water (3x 5.0 mL) and the combined aqueous layers were washed with toluene (6x 10 mL). The combined aqueous layers were concentrated to yield amine **10** (0.31 g, 0.85 mmol, 96%) as a colourless oil. DMF (2.1 mL, 0.20 M) and Et_3N (76 μL, 0.55 mmol, 1.3 equiv.) were added and the solution was cooled to 0 °C. Chloroacetyl chloride (44 μL, 0.55 mmol, 1.3 equiv.) was added dropwise and the mixture was stirred for 140 min. The mixture was evaporated to obtain an orange crude and purification by silica gel column chromatography (1:9, MeOH – DCM) yielded chloroacetamide **15** (0.14 g, 0.32 mmol, 77%) as pale yellow oil.

^{1}H NMR (400 MHz, $(CD_3)_2CO$) δ 7.72 (s, 1H, N*H*), 7.43 (s, 1H, N*H*), 4.08 (s, 2H, CH_2Cl), 3.96 (s, 2H, CH_2(C=O)), 3.70 – 3.52 (m, 18H, OCH_2), 3.43 – 3.37 (m, 6H, CH_2N_3, CH_2NH).

^{13}C NMR (101 MHz, $(CD_3)_2CO$) δ 170.6 (*C*=O), 166.8 (*C*=O), 71.4 (OCH_2), 71.3 (OCH_2), 71.1 (OCH_2), 71.0 (OCH_2), 71.0 (OCH_2), 70.9 (OCH_2), 70.8 (OCH_2), 70.6 (OCH_2), 70.6 (OCH_2), 70.4 (OCH_2), 70.2 (OCH_2), 69.9 (CH_2(C=O)), 51.2 (CH_2N_3), 43.3 (CH_2Cl), 40.2 (CH_2NH), 39.1 (CH_2NH).

***N*-(1-azido-10-oxo-3,6,12,15,18-pentaoxa-9-azaicosan-20-yl)-2-iodoacetamide**

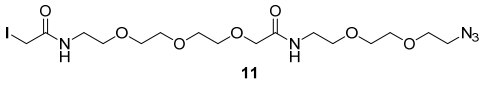

11

Chloroacetamide **15** (0.13 g, 0.30 mmol, 1.0 equiv.) was dissolved in acetone (2.9 mL, 0.10 M) and sodium iodide (0.14 g, 0.90 mmol, 3.0 equiv.) was added. The mixture was stirred for 48 hrs. The mixture was concentrated and purification by silica column chromatography (1:9, MeOH – DCM) yielded iodoacetamide **11** (0.11 g, 0.22 mmol, 72%) as pale yellow oil.

^{1}H NMR (500 MHz, $(CD_3)_2CO$) δ 7.79 (s, 1H, N*H*), 7.41 (s, 1H, N*H*), 3.99 (s, 2H, CH_2(C=O)), 3.76 (s, 2H, CH_2I), 3.70 – 3.59 (m, 14H, OCH_2), 3.56 (t, *J* = 5.7 Hz, 2H, CH_2CH$_2$NH), 3.52 (t, *J* = 5.5 Hz, 2H, CH_2CH$_2$NH), 3.45 – 3.38 (m, 4H, CH_2N_3, CH_2NH), 3.36 (q, *J* = 5.5 Hz, 2H, CH_2NH).

^{13}C NMR (126 MHz, $(CD_3)_2CO$) δ 170.7 (*C*=O), 168.4 (*C*=O), 71.4 (OCH_2), 71.2 (OCH_2), 71.2 (OCH_2), 71.0 (OCH_2), 71.0 (OCH_2), 70.9 (OCH_2), 70.6 (OCH_2), 70.2 (OCH_2), 70.0 (CH_2(C=O)), 51.3 (CH_2N_3), 40.5 (CH_2NH), 39.2 (CH_2NH), -0.2 (CH_2I).

References

(1) Bayer, E. Towards the Chemical Synthesis of Proteins. *Angew. Chem. Int. Ed. Engl.* **1991**, *30* (2), 113–129. https://doi.org/10.1002/anie.199101133.

(2) Merrifield, R. B. Solid Phase Peptide Synthesis. I. The Synthesis of a Tetrapeptide. *J. Am. Chem. Soc.* **1963**, *85* (14), 2149–2154. https://doi.org/10.1021/ja00897a025.

(3) Meldal, M. Pega: A Flow Stable Polyethylene Glycol Dimethyl Acrylamide Copolymer for Solid Phase Synthesis. *Tetrahedron Lett.* **1992**, *33* (21), 3077–3080. https://doi.org/10.1016/S0040-4039(00)79604-3.

(4) García-Ramos, Y.; Paradís-Bas, M.; Tulla-Puche, J.; Albericio, F. ChemMatrix® for Complex Peptides and Combinatorial Chemistry. *J. Pept. Sci.* **2010**, *16* (12), 675–678. https://doi.org/10.1002/psc.1282.

(5) van Geel, R.; Pruijn, G. J. M.; van Delft, F. L.; Boelens, W. C. Preventing Thiol-Yne Addition Improves the Specificity of Strain-Promoted Azide-Alkyne Cycloaddition. *Bioconjug. Chem.* **2012**, *23* (3), 392–398. https://doi.org/10.1021/bc200365k.

(6) Fairbanks, B. D.; Sims, E. A.; Anseth, K. S.; Bowman, C. N. Reaction Rates and Mechanisms for Radical, Photoinitated Addition of Thiols to Alkynes, and Implications for Thiol−Yne Photopolymerizations and Click Reactions. *Macromolecules* **2010**, *43* (9), 4113–4119. https://doi.org/10.1021/ma1002968.

(7) Merten, H.; Schaefer, J. V.; Brandl, F.; Zangemeister-Wittke, U.; Plückthun, A. Facile Site-Specific Multiconjugation Strategies in Recombinant Proteins Produced in Bacteria. *Methods Mol. Biol. Clifton NJ* **2019**, *2033*, 253–273. https://doi.org/10.1007/978-1-4939-9654-4_17.

(8) Karver, M. R.; Weissleder, R.; Hilderbrand, S. A. Bioorthogonal Reaction Pairs Enable Simultaneous, Selective, Multi-Target Imaging. *Angew. Chem. Int. Ed.* **2012**, *51* (4), 920–922. https://doi.org/10.1002/anie.201104389.

(9) Patterson, D. M.; Nazarova, L. A.; Xie, B.; Kamber, D. N.; Prescher, J. A. Functionalized Cyclopropenes As Bioorthogonal Chemical Reporters. *J. Am. Chem. Soc.* **2012**, *134* (45), 18638–18643. https://doi.org/10.1021/ja3060436.

(10) Späte, A.-K.; Bußkamp, H.; Niederwieser, A.; Schart, V. F.; Marx, A.; Wittmann, V. Rapid Labeling of Metabolically Engineered Cell-Surface Glycoconjugates with a Carbamate-Linked Cyclopropene Reporter. *Bioconjug. Chem.* **2014**, *25* (1), 147–154. https://doi.org/10.1021/bc4004487.

(11) Albin, T. J.; Tom, J. K.; Manna, S.; Gilkes, A. P.; Stetkevich, S. A.; Katz, B. B.; Supnet, M.; Felgner, J.; Jain, A.; Nakajima, R.; Jasinskas, A.; Zlotnik, A.; Pearlman, E.; Davies, D. H.; Felgner, P. L.; Burkhardt, A. M.; Esser-Kahn, A. P. Linked Toll-Like Receptor Triagonists Stimulate Distinct, Combination-Dependent Innate Immune Responses. *ACS Cent. Sci.* **2019**, *5* (7), 1137–1145. https://doi.org/10.1021/acscentsci.8b00823.

(12) Chan, M.; Kakitsubata, Y.; Hayashi, T.; Ahmadi, A.; Yao, S.; Shukla, N. M.; Oyama, S.; Baba, A.; Nguyen, B.; Corr, M.; Suda, Y.; Carson, D. A.; Cottam, H. B.; Wakao, M. Structure–Activity Relationship Studies of Pyrimido[5,4-b]Indoles as Selective Toll-Like Receptor 4 Ligands. *J. Med. Chem.* **2017**, *60* (22), 9142–9161. https://doi.org/10.1021/acs.jmedchem.7b00797.

(13) Kang, J. Y.; Nan, X.; Jin, M. S.; Youn, S.-J.; Ryu, Y. H.; Mah, S.; Han, S. H.; Lee, H.; Paik, S.-G.; Lee, J.-O. Recognition of Lipopeptide Patterns by Toll-like Receptor 2-Toll-like Receptor 6 Heterodimer. *Immunity* **2009**, *31* (6), 873–884. https://doi.org/10.1016/j.immuni.2009.09.018.

(14) Pavot, V.; Rochereau, N.; Rességuier, J.; Gutjahr, A.; Genin, C.; Tiraby, G.; Perouzel, E.; Lioux, T.; Vernejoul, F.; Verrier, B.; Paul, S. Cutting Edge: New Chimeric NOD2/TLR2 Adjuvant Drastically Increases Vaccine Immunogenicity. *J. Immunol.* **2014**, *193* (12), 5781–5785. https://doi.org/10.4049/jimmunol.1402184.

(15) Zom, G. G.; Willems, M. M. J. H. P.; Meeuwenoord, N. J.; Reintjens, N. R. M.; Tondini, E.; Khan, S.; Overkleeft, H. S.; van der Marel, G. A.; Codee, J. D. C.; Ossendorp, F.; Filippov, D. V. Dual Synthetic Peptide Conjugate Vaccine Simultaneously Triggers TLR2 and NOD2 and Activates Human Dendritic Cells. *Bioconjug. Chem.* **2019**, *30* (4), 1150–1161. https://doi.org/10.1021/acs.bioconjchem.9b00087.

(16) Pattabhi, S.; Wilkins, C. R.; Dong, R.; Knoll, M. L.; Posakony, J.; Kaiser, S.; Mire, C. E.; Wang, M. L.; Ireton, R. C.; Geisbert, T. W.; Bedard, K. M.; Iadonato, S. P.; Loo, Y.-M.; Gale, M. Targeting Innate Immunity for Antiviral Therapy through Small Molecule Agonists of the RLR Pathway. *J. Virol.* **2016**, *90* (5), 2372–2387. https://doi.org/10.1128/JVI.02202-15.

(17) Ramanjulu, J. M.; Pesiridis, G. S.; Yang, J.; Concha, N.; Singhaus, R.; Zhang, S.-Y.; Tran, J.-L.; Moore, P.; Lehmann, S.; Eberl, H. C.; Muelbaier, M.; Schneck, J. L.; Clemens, J.; Adam, M.; Mehlmann, J.; Romano, J.; Morales, A.; Kang, J.; Leister, L.; Graybill, T. L.; Charnley, A. K.; Ye, G.; Nevins, N.; Behnia, K.; Wolf, A. I.; Kasparcova, V.; Nurse, K.; Wang, L.; Puhl, A. C.; Li, Y.; Klein, M.; Hopson, C. B.; Guss, J.; Bantscheff, M.; Bergamini, G.; Reilly, M. A.; Lian, Y.; Duffy, K. J.; Adams, J.; Foley, K. P.; Gough, P. J.; Marquis, R. W.; Smothers, J.; Hoos, A.; Bertin, J. Design of Amidobenzimidazole STING Receptor Agonists with Systemic Activity. *Nature* **2018**, *564* (7736), 439–443. https://doi.org/10.1038/s41586-018-0705-y.

(18) van Moorsel, M. V. A.; Urbanus, R. T.; Verhoef, S.; Koekman, C. A.; Vink, M.; Vermonden, T.; Maas, C.; Pasterkamp, G.; Schiffelers, R. M. A Head-to-Head Comparison of Conjugation Methods for VHHs: Random Maleimide-Thiol Coupling versus Controlled Click Chemistry. *Int. J. Pharm. X* **2019**, *1*, 100020. https://doi.org/10.1016/j.ijpx.2019.100020.

(19) Tsukiji, S.; Nagamune, T. Sortase-Mediated Ligation: A Gift from Gram-Positive Bacteria to Protein Engineering. *ChemBioChem* **2009**, *10* (5), 787–798. https://doi.org/10.1002/cbic.200800724.

(20) Nguyen, G. K. T.; Wang, S.; Qiu, Y.; Hemu, X.; Lian, Y.; Tam, J. P. Butelase 1 Is an Asx-Specific Ligase Enabling Peptide Macrocyclization and Synthesis. *Nat. Chem. Biol.* **2014**, *10* (9), 732–738. https://doi.org/10.1038/nchembio.1586.

(21) Zhang, C.; Welborn, M.; Zhu, T.; Yang, N. J.; Santos, M. S.; Van Voorhis, T.; Pentelute, B. L. π -Clamp-Mediated Cysteine Conjugation. *Nat. Chem.* **2016**, *8* (2), 120–128. https://doi.org/10.1038/nchem.2413.

(22) Dai, P.; Zhang, C.; Welborn, M.; Shepherd, J. J.; Zhu, T.; Van Voorhis, T.; Pentelute, B. L. Salt Effect Accelerates Site-Selective Cysteine Bioconjugation. *ACS Cent. Sci.* **2016**, *2* (9), 637–646. https://doi.org/10.1021/acscentsci.6b00180.